NORTHWEST AFRICA 14446: A UNIQUE LUNAR DIMICT BRECCIA COMPOSED OF DISTINCT FELDSPATHIC CRYSTALLINE MELT BRECCIA LITHOLOGIES D. Sheikh[1], A. Ruzicka[1], M. Hutson[1], A. Greshake[2], E. Thompson[3], and P. Thompson[3], [1]Cascadia Meteorite Laboratory, Portland State University, Department of Geology, Portland, OR 97239, USA (dsheikh@pdx.edu), [2]Museum für Naturkunde Berlin, Invalidenstrasse 43, 10115 Berlin, Germany, [3]ET Meteorites, 16869 SW 65th Ave Suite #331, Lake Oswego, OR 97035, USA.

Introduction: The recent discoveries of unique feldspathic lunar meteorites [e.g. NWA 13531] have continued to provide additional research samples to the scientific community for better constraining the geologic diversity of the lunar surface not represented by the Apollo/Luna samples and other lunar meteorites [1-2]. Here, we report our preliminary results on Northwest Africa (NWA) 14446, a newly classified unique lunar feldspathic breccia.

History and Physical Characteristics: Northwest Africa 14446 was purchased from a meteorite dealer in Morocco on September 14th, 2021 by Edwin and Patrick Thompson. It represents a single 384 gram stone that measures 7 x 6 x 8 centimeters and displays no visible fusion crust. Visually in hand specimen NWA 14446 consists of a light-colored layer in the middle of the stone (~2.5 centimeters thick) that is sandwiched between two dark-colored layers, having the appearance of an elongated lithic clast or an intrusive dike structure (Fig. 1).

Fig. 1: *Hand specimen image of NWA 14446 stone.*

Petrography: Petrographic observation of NWA 14446 reveals two texturally distinct lithologies separated by a sharp boundary zone composed of broken up clasts, isolated mineral fragments, devitrified glass, and maskelynite.

Lithology 1 (light-colored layer, Fig. 2) represents a crystalline melt breccia composed of sub-angular feldspathic lithic clasts (Av. 1.0±0.2 mm diameter, n=11) and relict Mg-Al spinel grains (Mg#=68.9±0.8, Cr#=12.3±0.1, Av. 550±10 μm diameter, n=4) set within a microcrystalline matrix exhibiting a sub-ophitic texture composed of irregular olivine and pigeonite (some weakly zoned) grains and fractured and smooth plagioclase grains (some partially transformed into maskelynite) (silicate grain size Av. 100±40 μm diameter, n=51). Shock melt veins are visible throughout, some of which are associated with localized areas containing melt pockets, and some of which crosscut into the dark lithology. Accessory phases include ilmenite, apatite, troilite, and carbonate (from weathering veins).

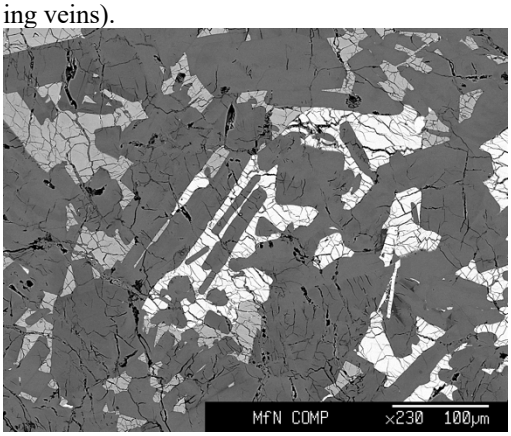

Fig. 2: *BSE image of light-colored layer (lithology 1).*

Lithology 2 (dark-colored layer, Fig. 3) represents a crystalline melt breccia composed of sub-angular feldspathic lithic clasts and isolated mineral fragments (Av. 190±90 μm diameter, n=51) set within a cryptocrystalline matrix exhibiting a sub-ophitic texture composed of irregular pyroxene, olivine, and plagioclase (some lath-like) grains (silicate grain size Av. 6.0±3 μm diameter, n=40). Some flow banding of matrix minerals is evident along clast boundaries. Accessory phases include ilmenite, apatite, troilite, kamacite, spinel, baddeleyite, and carbonate (from weathering veins). Some plagioclase grains in lithic clasts have been transformed into maskelynite.

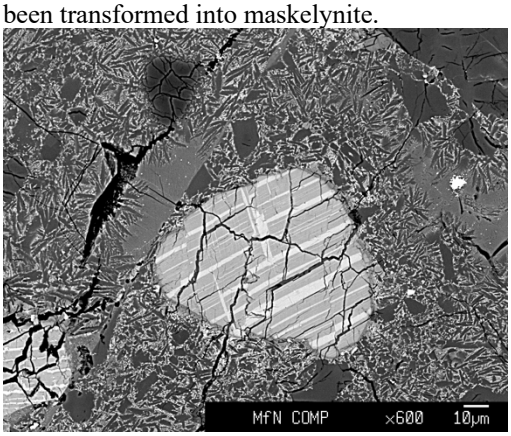

Fig. 3: *BSE image of dark-colored layer (lithology 2).*

A false color EDS + BSE chemical map containing both light and dark lithologies and the boundary zone separating them is displayed in Figure 4.

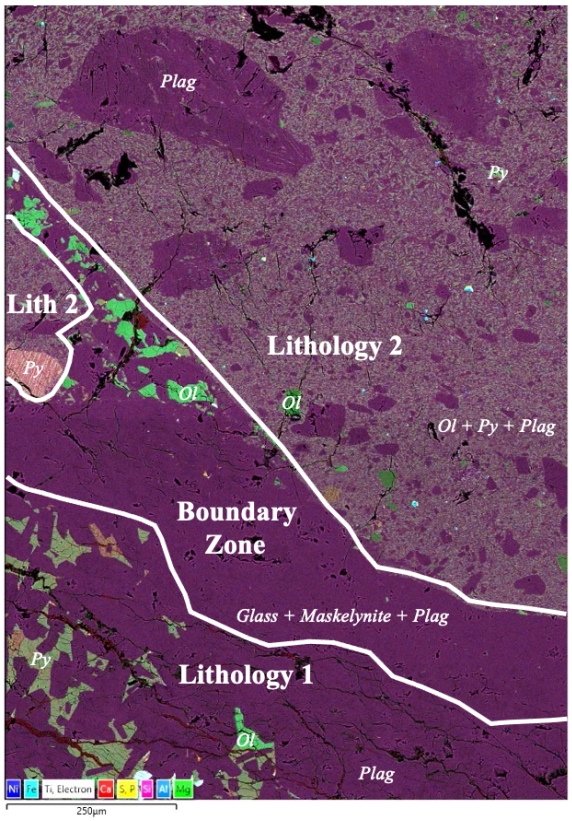

Fig. 4: *False color EDS + BSE chemical map of NWA 14446 containing both lithologies and the boundary zone outlined and labeled. Major mineral phases are labeled (Ol=olivine, Py=pyroxene, Plag=plagioclase). Element key and scale bar displayed.*

Mineral Chemistry: Mineral compositions reported for each lithology are displayed below.

Lithology 1: Olivine (Fa36.8±0.3, range Fa36.1-38.6, FeO/MnO=96±5, n=20), Pigeonite (Fs27.0±1.9 Wo12.7±3.4, range Fs23.8-31.6 Wo9.1-21.8, FeO/MnO=54±2, n=19), Augite (Fs48.4 Wo31.5, FeO/MnO=20, n=1), Calcic plagioclase (An97.0±0.6, range An96.1-97.9, n=15).

Lithology 2: Olivine (Fa29.5±4.4, range Fa17.9-38.6, FeO/MnO=94±14, n=21), Low-Ca Pyroxene (Fs32.5±17.1 Wo3.6±0.5, range Fs21.8-52.2 Wo3.2-4.1, FeO/MnO=58±4, n=3), Pigeonite (Fs36.8±15.3 Wo7.8±2.3, range Fs19.1-46.9 Wo6.5-10.5, FeO/MnO=56±3, n=3), Augite (Fs21.1±16.0 Wo34.1±11.4, range Fs9.8-32.4 Wo26.1-42.2, FeO/MnO=47±8, n=2), Calcic plagioclase (An96.4±1.9, range An92.3-98.8, n=12).

Averaged mineral compositions of olivine, pyroxene, and plagioclase from Lithology 1 and Lithology 2 are displayed in Figure 5. Mineral composition from Lithology 2 range from Ferroan Anorthosite (FAN) to Magnesian Anorthosite (MAN) compositions [3-4], indicative of Lithology 2 sampling a mixture of FAN and MAN-like material. Mineral compositions from Lithology 1 are relatively homogeneous and plot within the FAN field despite its similarly brecciated nature.

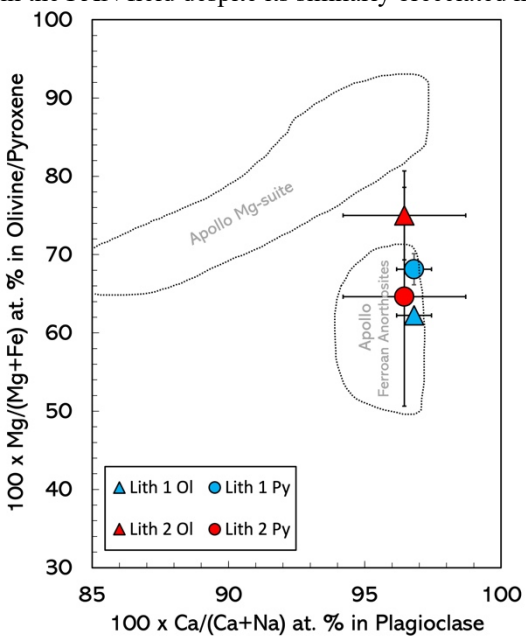

Fig. 5: *Averaged plagioclase An % vs. Olivine (triangles) and Pyroxene (circles) Mg# for Lithology 1 (blue) and Lithology 2 (red). Error bars represent 1σ standard deviation. Outlined FAN and Mg-suite fields taken from [3].*

Summary: Northwest Africa 14446 is composed of two different types of lithologies with distinctly different textures, representative of a lunar dimict breccia [5]. In this case, both lithologies are feldspathic crystalline melt breccias, unlike that found in most lunar breccias. Formation of this sample likely requires 1) the formation of Lithology 1 from impact melting and brecciation of a spinel-bearing anorthositic-like precursor, 2) injection of a later-generation impact melt containing regolith material, possibly into underlying, fractured basement rock composed of Lithology 1, and 3) partial melting of Lithology 1 and rapid crystallization of Lithology 2, forming the boundary zone.

Acknowledgements: Grant support from Oregon Space Grant Consortium (NASA award 80NSSC20M0035) is gratefully acknowledged.

References: [1] Ruzicka A. M. et al. (2021) *LPSC 52,* abstract #2234. [2] Korotev R. L. and Irving A. J. (2021) *MaPS, 56,* 206-240. [3] Goodrich C. A. et al. (1984) *JGR, 89*, C87-C94. [4] Gross J. et al. (2014) *EPSL*, 388, 318-328. [5] Stöffler D. et al. (1980) *Proc. Conf. Lunar Highlands Crust,* 51-70.